AsymBio

Application of the design of experiment to characterize depth filtration for bispecific antibody clarification

- QbD-driven clarification screening strategy for depth filtration
- Two-stage depth filter selection enabling high clarification capacity
- Key process parameters identified (pore size, charge, and feed flux of depth filter)
- Enhanced HCP removal with maintained product quality
- Improved robustness and performance of downstream clarification

Application of the design of experiment to characterize depth filtration for bispecific antibody clarification

Yunfei Pan, Min Li, Huoyan Hong, Kai Gao, Puya Zhao *

Shanghai AsymBio Biotechnology Co., Ltd., Building 8, No.12, Lane 855, Jinzheng Road, Jinshan Industrial Park, Shanghai, China

ARTICLE INFO

Keywords:
Clarification
Depth filtration
Risk assessment
Design of experiment
Design space
Process characterization

ABSTRACT

Depth filtration is crucial in the downstream process to clarify the cell culture fluid. With an increase in the upstream cell expression and cell density, achieving a high capacity of clarification (CLR) and the excellent removal of host cell proteins (HCPs) is an enormous challenge. We report a quality-by-design (QbD) case study of clarification screening to help understand the main functional relationships that link the process parameters to product quality or process attributes with prior process knowledge, risk assessment, and the design of experiment (DoE) approach. Our preliminary risk assessment showed that the pore size, charge, and inlet flux of the deep cassette significantly impacted clarification filtration. The DoE of the clarification capacity, protein purity, recovery, and HCP removal was conducted by selecting a two-stage depth filters (primary filters: 4070PC and S870PC; secondary filters: H0HP, H2HP, and H4HP) with different pore sizes, charge differences and inlet flow rates (100 / 200 LMH (L/m^2/h)). Depth filter encapsulation and the lower feed flux increased the filtration capacity and HCP removal, while other factors, such as pore size, affected the filtration process time and pressure and were not significant factors in terms of capacity and product quality. Our results suggest that these process parameters can effectively improve the overall performance of the downstream process.

1. Introduction

The global antibody therapy market is more than 200 billion in 2023. In recent years, it has emerged as a major category of new drugs developed. Antibody-related drugs with high specificity and low adverse effects show significant efficacy against a range of cancers and immune disorders (Donaghy, 2016; Lu et al., 2020). The Food and Drug Administration (FDA) has approved more than 100 antibody products to date, and antibody-related drugs dominate the pharmaceutical industry. An effective antibody therapy pipeline can provide the company with a higher revenue potential and give patients hope for survival. Pharmaceutical companies continuously optimize their production process platforms to meet market demands for larger scale, higher yield, and more efficient antibody production. Recent advancements in biotechnology, especially in the area of mammalian cell culture for biopharmaceutical production, have dramatically increased the titers. For example, high-throughput clonal screening has improved bispecific antibody (BsAb) expression, and product titers in cell culture often exceed 10 g/L (Majumdar et al., 2025). High-density cell expression generates massive amounts of biomass that need to be removed, and these high-density cultures pose a significant challenge to traditional clarification harvesting techniques (Almeida et al., 2021).

Typically, antibody clarification harvesting bridges upstream and downstream processes and is responsible for the removal of cells, cellular fragments, and other impurity aggregates. With advancements in technology, there is a wide selection of clarification technologies available for typical antibody harvesting, including centrifugation, tangential flow filtration (TFF) methods, and depth filtration. Depth filtration and centrifugation are the most widely used methods. However, both centrifugation and filtration techniques have limitations, as the increase in total cell density leads to elevated impurity levels in the cell culture solution. Centrifugal harvesting involves separation by centrifugal force based on the density and particle size characteristics in the mixture. During centrifugal harvesting, the feed inlet shear is high, adversely affecting the product quality. Removal of soluble impurities is difficult by centrifugal harvesting, often requiring bridging with depth filtration to provide a more clarified product for subsequent affinity chromatography (Roush and Lu, 2008; Gottschalk, 2017; Iammarino et al., 2007). TFF can handle high-expression cell cultures, and rapid polarization of the surface of the filter leads to longer processing time

* Corresponding author.
E-mail address: zhaopuya0522@asymchem.com.cn (P. Zhao).

https://doi.org/10.1016/j.cherd.2025.05.003
Received 13 December 2024; Received in revised form 25 April 2025; Accepted 1 May 2025
Available online 2 May 2025

and lower product recovery (Liu et al., 2014). Depth filtration, a widely applied cell harvesting technology, involves using primary filter pack-ages in series with secondary filter packages, which tend to have larger pore sizes and filter areas than secondary filter packages. Depth filtra-tion does remove cells, cell debris, and particulate contaminants and effectively removes soluble impurities, such as host cell proteins (HCPs) and host cell DNA (HCD) (Singh et al., 2013). The depth filter layer is prepared with fibrous material, such as cellulose or polypropylene, as the main structure and is combined with the filter aid through positively charged bonds to create a flat sheet. The clarification mechanisms involved in depth filtration (as shown in Fig. 1) are based on direct size-based interception, deposition of particles in the tortuous apertures within the filter, and adsorption based on mixed-mode interactions, such as hydrophobicity and electrostatic forces (Shukla and Suda, 2017).

Depth filtration is currently mostly for single-use, reducing the risk of cross-contamination in production. The cases on clarification with depth filtration explored in most studies rely mainly on mechanistic models of depth filtration operations. For example, the difference in binding ca-pacity of positively charged proteins between traditional and synthetic depth filters was analyzed previously and compared based on static binding capacity measurements (Nguyen et al., 2018). Comparative experiments demonstrated that the depth filter's capacity affected the capability of removing HCP (Yigzaw et al., 2006), and screening of different filters demonstrated the effectiveness of positively charged filters for HCD removal (Charlton et al., 1999).

Different properties of depth filters characterize Chinese hamster ovary (CHO) cells and show a 10-fold difference in capacity and turbidity, indicating that the characteristics of cell suspension and depth filters influence the process properties (Nejatishahidein and Zydney, 2021). The quality-by-design concept is widely used in the pharma-ceutical industry to characterize each unit operation of a process. However, few cases of clarified depth filter harvesting for investigating the impact of process parameters on product quality or process attri-butes is documented in the literature. The QbD concept is a systematic approach to development that begins with predetermined goals and emphasizes process understanding and process control. QbD is defined in the ICH (International Council for Harmonisation of Technical Re-quirements for Pharmaceuticals for Human Use) Q8 guideline as a process that begins with a pre-defined product goal, is based on a sci-entific and risk management approach, enhances product and process understanding and process control, and investigates the relationship between product quality attributes, raw material quality attributes, and process parameters through rationalized design of experiments. A design space (DS) is established that meets predefined objectives and is process-robust under multiple response variables. Quality risk management is performed based on the DS to establish a pharmaceutical quality control strategy.

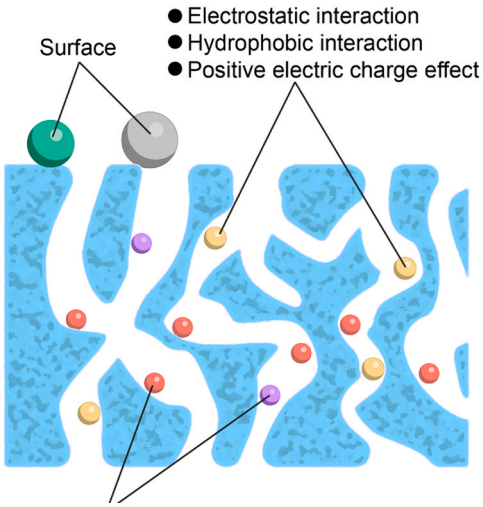

Fig. 1. Schematic representation of depth filtration.

We report a QbD case study of clarification screening to help understand the main functional relationships that link the process parameters to product quality or process attributes with prior process knowledge, risk assessment, and the DoE approach.

2. Material and methods

2.1. Cell culture and protein expression

Cell culture suspensions were derived upstream from CHO cells expressing bispecific antibody molecules in 2 L or 10 L bioreactors running in the batch mode. The cell culture suspensions were collected after 15 days of incubation and harvested when the cell density reached 20×10^6 cells/mL with approximately 90 % cell viability. The titer was 6.78 g/L, the solid content of the supernatant was about 10 %, and turbidity was > 5000 NTU (a 1:10 dilution with buffer for BsAb 5250 NTU). The cell culture fluid (CCF) was filtered using two-stage serial depth filters. Filters were purchased from Hangzhou Cobetter Filtration Co., Ltd. The primary depth filters included 4070PC and S870PC. The secondary depth filters included H0HP, H2HP, and H4HP. All the depth filtration filter area was 23 cm^2. The materials of construction of depth filter are shown in Table 1, and the pore size of different filters is shown in Table 2.

2.2. Risk assessment

Risk Priority Number (RPN) was calculated using the Failure Mode and Effects Analysis (FMEA) tool as shown below (Liu et al., 2019).

RPN = Severity (S) x Occurrence (O) x Detectability (D).

The severity, occurrence, and detectability of each process parameter were scored based on available literature or experimental data according to the risk assessment criteria shown in Table 3 and risk assessment determination shown in Tables 4, 5, and 6.

Based on the RPN results, the process parameters were classified, and accordingly, the experimental strategy was established, as shown in Table 7.

2.3. DoE screening study design and data analysis

The multivariate study was performed with one factor at 3 levels and two factors at 2 levels, namely feed flux, the type of primary depth filter, and the type of secondary depth filter. These three factors were investigated in a full factorial design, resulting in 12 experiments and 6 center points. The full factorial design was chosen because it supports linear effects and all interactions, so each factor can be evaluated separately. The experimental design is shown in Table 8 and Fig. 2.

After the optimization experimental series was complete, the results of each experimental point were entered in JMP® (18) software to obtain optimal factor settings for the process. The evaluation involved a statistical analysis of the data generated.

Table 1
Materials of construction of depth filter.

Module	Materials of construction
Membranes	Cellulose, Kieselguhr, Synthetic resin
Cages	Polypropylene
Screw Cap	Glass Fiber Reinforced PP
Plastic Parts	Polypropylene

Table 2
Pore size of different depth filters.

Depth filter	Pore size (μm)
4070PC	4–18
S870PC	0.1–9
H2HP	0.01–0.2
H4HP	0.01–0.1
H0HP	0.02–0.2

Table 3
Risk assessment criteria.

S	Severity
Low (L)	It has little or no impact on the key quality attributes or parameters of the product and rarely impacts the quality of the product.
Medium (M)	It has a certain impact on the key quality attributes or parameters of the product and indirectly affects the product quality.
High (H)	It has a very significant impact on the key quality attributes or parameters of the product, which directly affects the product quality.
O	**Occurrence**
Low (L)	It is almost impossible
Medium (M)	Occurs occasionally
High (H)	Recurring or unavoidable
D	**Detectability**
Low (L)	When it occurs, it is rare and hard to detect.
Medium (M)	Once it has occurred, it can be detected by certain control measures.
High (H)	Once it occurs, it is always detectable.

Table 4
Risk assessment determination based on severity and occurrence.

Risk Level	Severity			
Occurrence	L	M	H	
	L	L	L	M
	M	L	M	H
	H	M	H	H

Table 5
Risk assessment determination based on detectability and risk level.

RPN		Detectability		
		H	**M**	**L**
Risk Level	**L**	L	L	M
	M	L	M	H
	H	M	H	H

Table 6
Risk assessment description.

RPN	Risk Assessment Description
L	Acceptable risk without the need to take an action
M	Non-critical risks, which are acceptable, and steps should be taken to reduce the risk
H	Critical risks, with actionable measures required to reduce them

Table 7
RPN classification and corresponding experimental strategy.

RPN	Experimental Strategy
L	Univariate (OFAT), if required
M	Multivariate (DoE) or Univariate (OFAT)
H	Multivariate (DoE)

Table 8
The experimental study design.

Exp No.	Run Order	Feed Flux (LMH)	Type of Primary Depth Filter[1]	Type of Secondary Depth Filter[2]
1	14	100	−1	1
2	1	100	−1	2
3	10	100	−1	3
4	8	100	1	1
5	5	100	1	2
6	6	100	1	3
7	11	200	−1	1
8	9	200	−1	2
9	13	200	−1	3
10	7	200	1	1
11	15	200	1	2
12	2	200	1	3
13	16	150	−1	2
14	17	150	−1	2
15	18	150	−1	2
16	3	150	1	2
17	4	150	1	2
18	12	150	1	2

[1] "-1" and "1" primary depth filters represent 4070PC and S870PC, respectively; [2] "1," "2," and "3" secondary depth filters represent H0HP, H2HP, and H4HP, respectively.

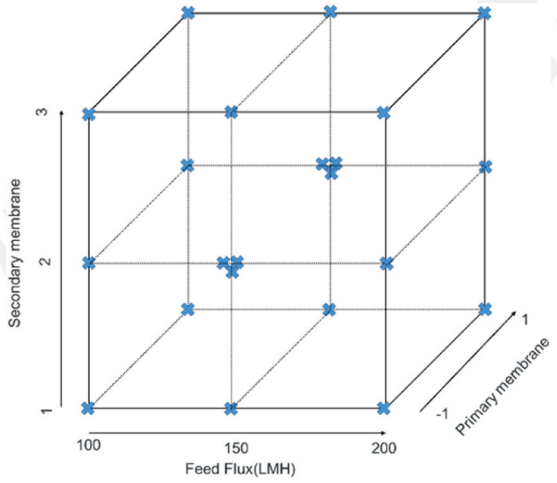

Fig. 2. Schematic representation of the conducted design of experiments for the feed flux, primary filter, and secondary filter. Primary filter: "-1" stands for "4070PC"; "2" stands for "S870PC"; Secondary filter: "1"stands for "H0HP" ; "2" stands for "H2HP" ; "3" stands for "H4HP".

2.4. Depth filter and depth filtration

Filtration experiments were performed using an area ratio with a 3:1 depth filter. The inlet flow rate of the clarification was calculated according to the secondary depth filtration filter, and the inlet flow rate of 150 LMH was used to equilibrate the depth filtration filters before sample loading. The performances of different depth filtration filter combinations at flow rates of 100 LMH and 200 LMH were tested every 10 minutes (the delta pressure of the cassette and the turbidity of the harvested liquid were tested). The turbidity of 20 NTU was used as the filter loading endpoint. The HCP, HCD, titer, turbidity, and protein purity of the clarified harvest were detected after completing experiment, and then the yield was calculated.

2.5. HCP analysis

HCP was detected using a sandwich enzyme-linked immunosorbent assay (ELISA) with the Cygnus CHO Host Cell Proteins 3rd generation kit. The 50 μL sample was to be tested, and 150 μL of α-CHO was taken.

Horseradish Peroxidase (HRP) was added to the coated 96-well microtiter strips and incubated at 400–500 rpm for 2 hours. The strips were washed with 1X washing buffer thrice, using 300 μl each time. Next, 100 μL of TMB color-developing solution was added, and the sample was incubated away from light for 2 hours. Finally, 50 μL of the stop solution was added, and a microplate reader was used to obtain optical density (OD) values at 450–650 nm.

2.6. Titer analysis

ChromaX@A20, 2.1 mm× 30 mm (Bio-Link, cat.2821–1111) was used to determine the titer. The mobile phase A comprised 1X phosphate buffered saline (PBS), pH 7.2. The mobile phase B comprised 0.1 mol/L Sodium acetate (NaAc) - Acetic Acid (HAc), pH 3.0. The injection volume was 50 μL for each sample. Elution was performed isocratically at 1 mL/min. After using the EMPOWER integration process, the peak area was used as the ordinate. The concentration was used as the abscissa, and the EMPOWER was used to plot a linear standard curve. The peak area of each sample was automatically calculated using the regression equation curve.

2.7. SEC-HPLC analysis

AdvanceBio Sections 300A, 2.7 μm, 7.8 mm × 300 mm (Agilent Technologies, cat. 0006663018–18) was used for size exclusion high-performance liquid chromatography (SEC-HPLC). The mobile phase comprised 0.1 mol/L sodium phosphate, 0.25 mol/L NaCl, and 5 % isopropanol at pH 6.8. The injection volume of BsAb was 50 μg for each sample. Elution was performed isocratically at 0.8 mL/min at 30°C, and protein elution was monitored by ultraviolet absorption at 280 nm.

3. Results and discussion

3.1. Risk assessment

3.1.1. Criticality assessment of process parameters

Following the ICH8 (R2) guidelines, the criticality of process parameters was assessed to prioritize the list of potential critical process parameters (pCPPs) or potential key process parameters (pKPPs). The severity, occurrence, and detectability of each process parameter were assessed. The overall results are summarized in Table 9.

Based on knowledge of the production process evaluation, some process parameters were evaluated in regard to their importance for the process and theoretical risks for further downstream processing.

Cell viability and cell density were determined as critical parameters for process recovery (Wohlenberg et al., 2022), and assessed as medium. The occurrence was assessed as low, and detectability was assessed as high due to the easy detectability of cell viability and density, and daily monitoring.

The inlet pressure was directly affected by the feed flux, and the shear force was affected, which might have resulted in aggregation (Wee et al., 2020). Therefore, the severity of feed flux was assessed as high. Considering that the feed flux was monitored in the whole process but only detected before the study, the occurrence was assessed as low, and detectability was assessed as medium.

As for different primary and secondary depth filters, Ohnmar Khanal *et al (*Khanal et al., 2018*)*. have reported that properties, such as surface area, morphology, surface charge density, and composition, as well as filter fineness, contribute differently to impurity clearance and process recovery reduction. Thus, the severity of the type of primary and secondary depth filters was assessed as high. Because the type of primary and secondary depth filters was checked multiple times when the clarification process started while properties of depth filters could not be detected during the process, the occurrence and detectability were both assessed as low.

3.1.2. Experimental strategy of process parameters

The efficiency of clarification is related to the cell viability and density of loading, and cell culture suspensions with lower cell viability contain a large amount of HCP and cell debris, which increases the risk of plugging the depth filter. Higher cell densities will increase the pressure during filtration; cell density and viability are determined by upstream culture conditions and are not involved in the experimental strategy. In addition, the feed flux and the kind of depth filter are also important process parameters for the experiment, which directly affect the pressure, capacity, HCP, etc., during filtration. For example, higher flow rates may lead to higher pressures in the stream during filtration, then cells can break up and release more HCP impurities, etc.; the lower feed flux increases the residence time of the material in the processing cell. The charge and pore size of the depth filter directly reflect the interception of impurities. Based on this information and Table 3, we performed a risk assessment and summarized it in Table 9.

RPN was applied as the basis for assessing the required level of experimental complexity and strategy for the clarification process characterization study. The experimental strategy established for each process parameter is summarized in Table 9, following the information stated in Table 7.

3.2. Experimental results of process pressure, capacity, feed time, HCP reduction, protein purity and yield

The difference between the primary and secondary filters is reflected in the filter surface charge and filter pore size. To accurately analyze the effect of different filter selections on clarification filtration, the filter pore size and filter charge were subsequently normalized according to the proportionality between the filter packets for the final model fitting and analysis of results. As shown in Table 10, “40” and “1” of the primary depth filter represent the pore size of 4070PC and S870PC, respectively, and “1” and “1.67” represent the charge of 4070PC and S870PC, respectively. Similarly, “4,” “2,” and “1” of the secondary depth filter represent the pore size of H0HP, H2HP, and H4HP, respectively, and “0,” “1,” and “1.2” represent the charge of H0HP, H2HP, and H4HP, respectively.

In order to evaluate the practicability of clarification, the responses of delta pressure of filters (primary filter and secondary filter), as well as loading capacity, yield and feed time were analyzed. These attributes can have a severe effect on the expenses of the clarification step and the following chromatographic steps. Additionally, the SEC-HPLC purity (high molecular weight (HMW) and monomer) and HCPs reduction were analyzed as its main critical quality attributes (CQA) which represents the quality of sample during clarification. The results of the responses mentioned above are all listed in Table 10.

Table 9
Criticality assessment and experimental strategy of process parameters.

Process parameters	Severity	Occurrence	Detectability	RPN	Experimental strategy
Cell viability of loading	M	L	H	L	Not required
Cell density of loading	M	L	H	L	Not required
Feed flux	H	L	M	M	DoE
Kind of primary depth filter	H	L	L	H	DoE
Kind of secondary depth filter	H	L	L	H	DoE

Table 10
Results of primary filter delta pressure, secondary filter delta pressure, capacity, HCP reduction, feed time, and protein purity (HMW and Monomer).

Input						Output							
Group	Feed Flux (LMH)	Primary filter charge	Primary filter pore size	Secondary filter charge	Secondary filter pore size	Primary filter Δ pressure (bar)	Secondary filter Δ pressure (bar)	Capacity (L/m^2)	HCPs Reduction (%)	Time (min)	HMW (%)	Monomer (%)	Yield (%)
−12	100	1.00	40	1	2	0.50	0.35	180	86	109	5.78	92.45	90
+ 23	200	1.67	1	1.2	1	1.50	0.80	200	60	81	5.99	92.24	93
+ 20	150	1.67	1	1	2	0.88	0.55	190	62	89	6.22	91.81	87
+ 20	150	1.67	1	1	2	0.83	0.44	210	64	93	5.98	92.55	94
−22	100	1.67	1	1	2	0.76	0.41	240	83	144	5.32	92.79	95
−23	100	1.67	1	1.2	1	1.10	0.60	230	72	134	5.45	92.53	93
+ 21	200	1.67	1	0	4	0.70	0.30	160	30	67	5.54	92.51	94
−21	100	1.67	1	0	4	0.50	0.00	200	64	118	6.12	92.11	96
+ 12	200	1.00	40	1	2	0.77	0.50	150	49	66	4.99	92.87	95
−13	100	1.00	40	1.2	1	0.95	0.60	220	85	122	4.65	93.30	92
+ 11	200	1.00	40	0	4	0.15	0.10	100	23	38	5.45	92.77	89
+ 20	150	1.67	1	1	2	0.82	0.49	190	59	88	5.67	93.15	89
+ 13	200	1.00	40	1.2	1	1.25	0.85	170	44	79	5.44	92.77	91
−11	100	1.00	40	0	4	0.35	0.20	180	55	111	5.19	92.98	96
+ 22	200	1.67	1	1	2	0.80	0.35	180	44	55	5.42	92.70	96
−10	150	1.00	40	1	2	0.75	0.54	160	53	99	5.98	93.01	93
−10	150	1.00	40	1	2	0.70	0.49	170	59	92	5.63	92.56	92
−10	150	1.00	40	1	2	0.67	0.42	170	61	95	5.61	92.82	89

Generally, were available, predefined acceptance limits of the responses for modelling are summarized in Table 11. The following seven study outcomes could be categorized as two types. The case type determination is based on whether the responses values are lying in the accepted range specified for the clarification process. The type I is the difference between the maximum and minimum values of the outcomes inside the specification. The type II is opposite, that is to say, the difference between the maximum and minimum values of the outcomes outside the specification. Responses of primary filter Δ pressure, secondary filter Δ pressure, capacity, HCPs reduction, feed time all belonged to type I. While both protein purity (HMW and Monomer) and yield were of the opposite type (type II).

3.3. Statistical analysis of process pressure, capacity, feed time, HCP reduction, protein purity and yield

Statistical analysis was conducted on the responses which were of type I including primary filter delta pressure, secondary filter delta pressure, capacity, HCP reduction, and feed time. JMP® (18) software was applied for statistical analysis and a least squares fitting algorithm was used to obtain a good model for delta pressure of the primary filter ($R^2 = 0.93$, model p-value < 0.0001), delta pressure of the secondary filter ($R^2 = 0.84$, model p-value < 0.0001), capacity ($R^2 = 0.86$, model p-value < 0.0001), feed time ($R^2 = 0.88$, model p-value < 0.0001), and HCP reduction ($R^2 = 0.90$, model p-value < 0.0001). The results of the statistical analysis are shown in Fig. 3.

For further in-depth investigation of the varied process parameter effects and interactions, various critical responses of the process step were analyzed.

Table 11
Predefined acceptance limits of the responses for modelling.

Responses	Predefined acceptance limits of the responses
Primary filter delta pressure (bar)	> 0.2
Secondary filter delta pressure (bar)	> 0.2
Capacity (L/m^2)	> 20
HCPs Reduction (%)	> 10
Time (min)	> 10
Protein purity (HMW and Monomer) (%)	> 2
Yield (%)	> 10

3.3.1. Process pressure

Several biotechnology methods have been developed to achieve a dramatic increase in titer, such as intensified fed-batch, with advancements in cell culture production. However, potential impurities and dead cells also concomitantly increase. A fairly high solid content or turbidity suggests massive amounts of dead cells and debris, which can cause excessive pressure of depth filtration.

In this study, a challenging feed liquid was investigated, and its solid content (10 %) was 2–3 times that of the conventional fluid. We studied the effect of the pore meridian and charge of the depth filtration filter and the feed flux on the pressure. The pressure of the primary filter was negatively correlated with the pore size (p-value = 0.00003) and the charge (p-value = 0.00126) of the secondary filter. The pore size of the primary filter was negatively correlated (p-value = 0.00075) and the feed flux was positively correlated (p-value = 0.00642). There was an interaction between feed flux and secondary filter pore size. The pressure of the secondary filter was negatively correlated with the pore size of the secondary filter (p-value = 0.00000) and the feed flux was positively correlated (p-value = 0.03266) (Fig. 3). The pore size of the secondary filter was the main factor affecting the pressure of the depth filters, suggesting that the increase in pore size allows the filter to hold more cell debris and HCP. Particles smaller than the pores cannot form filter cakes on the surface of the filter media, and these particles enter the media, approach the wall of the pores by inertia and diffusion, and are deposited under the action of static electricity, so as to separate from the fluid. Depth filtration will gradually shrink the pores inside the filter media and will gradually clog. The smaller pore size, the greater the resistance of the filter to the passage of the fluid, and the greater the pressure required for the fluid to pass through. When filtering cell suspensions with small pore sizes, the filters are more likely to be clogged by particles, making it more difficult for fluid to pass through after blockage, further increasing resistance. The small aperture limits the amount of fluid passing through per unit time, and when the fluid passes through the small aperture, the pressure drop increases, resulting in an increase in the filter pressure. Therefore, increasing the pore size of the primary and secondary filters can facilitate the control of clarification pressures at lower safe levels. The differential pressure of H4HP exceeded 1.0 bar during the experiment, far above the pressure endpoint, might be due to the pore size of the H4HP flow channel was small, so the model of H4HP was not studied subsequently.

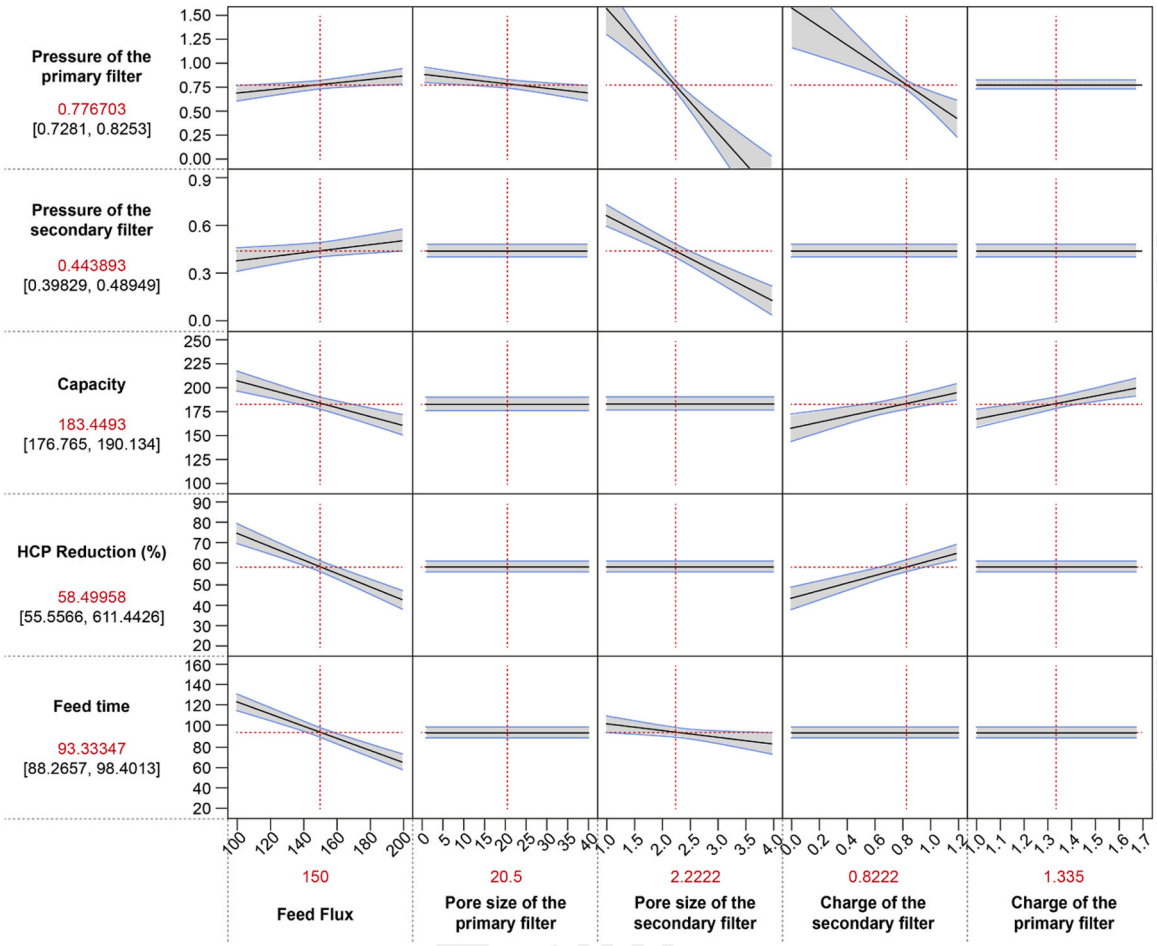

Fig. 3. Prediction profiler depiction of changes in the process pressure / capacity / feed time / HCP reduction as a function of the factors studied in the DoE.

3.3.2. Capacity

The charge of the primary filter (p-value = 0.00011) and the secondary filter (p-value = 0.00054) positively affected the capacity (Fig. 3). The charge in the depth filter enhanced the adsorption of HCP and cellular debris and prevented a rapid increase in pressure and turbidity during the process. As shown in Fig. 3, feed flux negatively affected the capacity (p-value =0.00003). The capacity of the clarification decreased as the feed flux increased. The filter cavity was rapidly blocked by the cell debris and particles when the feed flux reached 200 LMH. Therefore, increasing the charge of the depth filters and appropriately reducing the feed flux can effectively improve the filter capacity during the clarification process of high-density cell culture supernatant.

3.3.3. Feed time

Considering the stability of the target protein and the convenience of further scale-up, generally, the feed time should be better controlled within 2 hours. Both the feed flux (p-value = 0.00000) and pore size of the secondary filter (p-value =0.03059) negatively affected the feed time, especially the feed flux (Fig. 3). The loading process took about 80 minutes when the feed flux reached 200 LMH. Nevertheless, it took over 2 hours to load the sample when the feed flux was reduced to 100 LMH. There was a risk that the product would be restored when the filtration time exceeded 2 hours. The influence of feed flux on capacity and feed time should be balanced, and the most suitable feed flux was 150 LMH in this case.

3.3.4. HCP reduction

The feed flux (p-value = 0.00000) was inversely related to HCP removal capability, showing a high correlation (Fig. 3). The retention time between the feedstock and filters increased significantly with the decrease of the feed flux, whereas the clarification removed the soluble impurities mainly through non-specific adsorption (electrostatic or hydrophobic). The increase in the retention time allowed the feedstock to fully contact the depth filter cavity and effectively trap HCPs. While the charge of the secondary filter (p-value = 0.00002) was positively related to HCP removal (the value of log reduction value (LRV)), the higher the charge of the depth filter, the stronger the ionic interaction it exhibited, and the more the soluble proteins (HCPs) adsorbed. Therefore, reducing the inlet flux and selecting depth filters with larger charges can provide better HCP removal performance.

3.3.5. Purity (SEC-HPLC) and yield

The tested process parameters of depth filtration showed no significant effects on aggregates, monomers, and the yield. As shown in Table 10, the change rate of monomer purity in all experimental groups was within 2 % compared with the loading sample, indicating that different process parameters of these experiments did not affect the stability of the target protein (polymerization or reduction). However, different bispecific antibodies tended to show variable stability as well as pressure feedback, and thus, the influence of depth filtration on the purity of the proteins should be considered.

The initial raw data of the yield showed that this response was robust because all measured values of the recovery were within the range of 87 % - 96 % (difference less than 10 %). It means the yield would not be affected significantly by the tested range of the process parameters. The inapparent variation in the process yield might be due to the fact that the tested depth filters were predominantly positively charged or uncharged, resulting in less target protein adsorption. If the ionic

composition of depth filters is more complex, the recovery might be unexpectedly influenced. Furthermore, the recovery might also be impacted by the cell density, cell viability as well as solid content of upstream cell culture fluid. The variety of depth filters and diversity of cell culture could be regarded as another direction of study on the step of clarification.

3.3.6. *Design space*

The challenge of depth filtration due to the high expression of bispecific monoclonal antibodies requires a robust and efficient clarifying filtration process, and the overall processing design needs to consider filtration pressure, filtration time, and the ability of impurity removal.

Combined with the clarification filtration requirements of bispecific antibody platforming, and to ease the process scale-up, the process performance and product quality of clarification filtration need to be controlled within a certain range. And the following requirements are generally recommended: delta pressure of the primary filter $\leq$ 0.8 bar, delta pressure of the secondary filter $\leq$ 1.0 bar, secondary filter capacity $\geq$ 150 L/m^2, reduction of HCPs $\geq$ 50 %, the feed time $\leq$ 120 min, and yield $\geq$ 85 %.

Based on these requirements of clarification process, the final output design space was generated in Fig. 4, wherein the output range of primary filter pore size is 30–40 (that is 3–4 μm), the output range of primary filter charge is 1.00–1.67, the output range of secondary filter pore size is 2–2.6 (that is 0.2–0.26 μm), the output range of secondary filter charge is 0.9–1.2, and the output range of inlet flow rate is 107–150 LMH. Within this process range, the process pressure and filtration duration can be effectively controlled and simultaneously it can ensure high loading capacity, good yield, and excellent HCP reduction. Although most commercially available depth filters have fixed pore size and charge; in such a case, we could still choose 4070PC as the primary depth filter and H2HP as the secondary depth filter, then control the inlet flow rate within the range of 107–150 LMH, the process requirements were all met. Therefore, based on the results of this investigation, the appropriate depth filters according to the different fermentation broths can be effectively selected.

4. Conclusion

In summary, we investigated some potential critical or key process parameters of clarification based on DoE. The pore size of the secondary depth filter could affect the pressure during the sample loading process within a certain range but had no significant effect on the capacity. An appropriate inlet flow flux required a balance between process efficiency and HCP removal performance. The charge of the deep filter could provide electrostatic interaction with HCPs and profoundly affect the HCP removal performance in a cell suspension with high cell density and turbidity. Accordingly, a series of depth filter combinations were chosen, and some crucial parameters were optimized by designing a spatial model. The findings can guide the process for high-density filtration and low-viability cell culture mediums.

Abbreviations

BsAb: Bispecific Antibody; CCF: cell culture fluid; CHO: Chinese hamster ovary; CLR: clarification; CQA: critical quality attributes; D: detectability; DoE: design of experiment; DS: design space; ELISA: enzyme-linked immunosorbent assay; FDA: Food and Drug Administration; FMEA: failure mode and effects analysis; H: high; HAc: Acetic Acid; HCD: host cell DNA; HCP: host cell protein; HMW: high molecular weight; HRP: Horseradish Peroxidase; ICH: International Council for Harmonisation of Technical Requirements for Pharmaceuticals for Human Use; L: low; LMH: L/m^2/h; M: medium; NaAc: Sodium acetate; LRV: log reduction value; O: occurrence; OD: optical density; PBS: phosphate buffered saline; pCPPs: potential critical process parameters; pKPPs: potential key process parameters; QbD: quality-by-design; RPN: risk priority number; S: severity; SEC-HPLC: size exclusion high-performance liquid chromatography; TFF: tangential flow filtration;

CRediT authorship contribution statement

Hong Huoyan: Writing – original draft, Resources, Methodology, Formal analysis. **Li Min:** Writing – review & editing, Formal analysis, Conceptualization. **Pan Yunfei:** Writing – review & editing, Writing – original draft. **Zhao Puya:** Writing – review & editing, Conceptualization. **Gao Kai:** Writing – review & editing.

Consent for publication

Not applicable.

Ethics approval and consent to participate

Not applicable.

Funding

Not applicable.

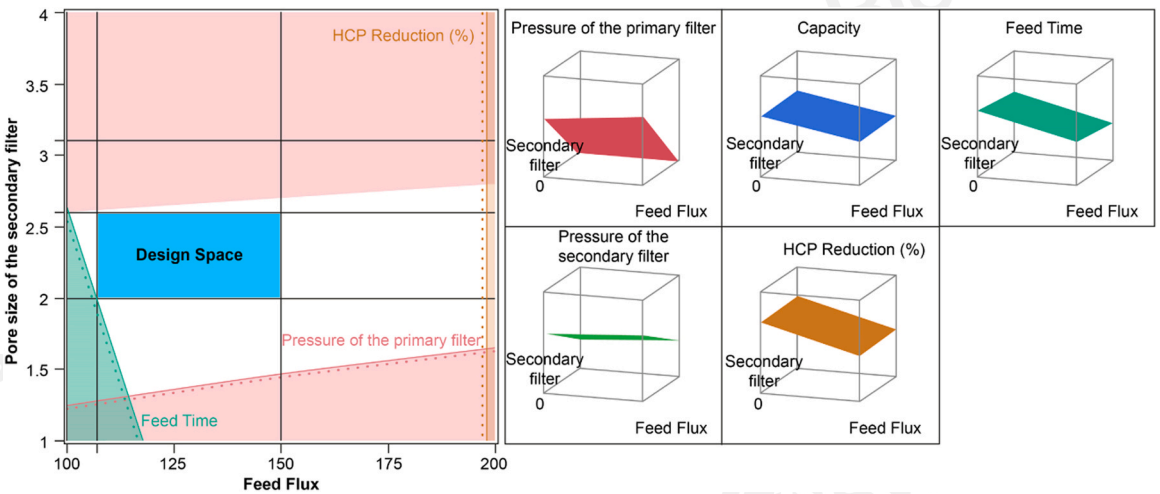

Fig. 4. Design space based on process requirements.

Declaration of Competing Interest

The authors declare that they have no competing interests

Acknowledgements

Not applicable.

Data availability

All data generated or analyzed during this study are included in this article.

References

Donaghy, H., 2016. Effects of antibody, drug and linker on the preclinical and clinical toxicities of antibody-drug conjugates. mAbs 8, 659–671. https://doi.org/10.1080/19420862.2016.1156829.

Lu, R.-M., Hwang, Y.-C., Liu, I.J., Lee, C.-C., Tsai, H.-Z., Li, H.-J., et al., 2020. Development of therapeutic antibodies for the treatment of diseases. J. Biomed. Sci. 27. https://doi.org/10.1186/s12929-019-0592-z.

Majumdar, S., Desai, R., Hans, A., Dandekar, P., Jain, R., 2025. From efficiency to yield: exploring recent advances in CHO cell line development for monoclonal antibodies. Mol. Biotechnol. 67. https://doi.org/10.1007/s12033-024-01060-6.

Almeida, A., Chau, D., Coolidge, T., El-Sabbahy, H., Hager, S., Jose, K., et al., 2021. Chromatographic capture of cells to achieve single stage clarification in recombinant protein purification. Biotechnol. Prog. 38. https://doi.org/10.1002/btpr.3227.

Roush, D.J., Lu, Y., 2008. Advances in primary recovery: centrifugation and membrane technology. Biotechnol. Prog.

Gottschalk, U., 2017. Preocess Scale Purification of Antibodies. John Wiley & Sons, Inc.

Iammarino, M., Nti-Gyabaah, J., Chandler, M., Roush, D., Goklen, K., 2007. Impact of Cell Density and Viability on Primary Clarification of Mammalian Cell Broth. BioProcess International.

Liu, H.F., Ma, J., Winter, C., Bayer, R., 2014. Recovery and purification process development for monoclonal antibody production. mAbs 2, 480–499. https://doi.org/10.4161/mabs.2.5.12645.

Singh, N., Pizzelli, K., Romero, J.K., Chrostowski, J., Evangelist, G., Hamzik, J., et al., 2013. Clarification of recombinant proteins from high cell density mammalian cell culture systems using new improved depth filters. Biotechnol. Bioeng. 110, 1964–1972. https://doi.org/10.1002/bit.24848.

Shukla, A.A., Suda, E., 2017. Harvest and recovery of monoclonal antibodies: cell removal and clarification. Preocess Scale Purification of Antibodies. John Wiely & Sons, Inc, USA.

Nguyen, H.C., Langland, A.L., Amara, J.P., Dullen, M., Kahn, D.S., Costanzo, J.A., 2018. Improved HCP reduction using a new, all-synthetic depth filtration media within an antibody purification process. Biotechnol. J. 14. https://doi.org/10.1002/biot.201700771.

Yigzaw, Y., Piper, R., Tran, M., Shukla, A.A., 2006. Exploitation of the adsorptive properties of depth filters for host cell protein removal during monoclonal antibody purification. Biotechnol. Prog. 22, 288–296. https://doi.org/10.1021/bp050274w.

Charlton, H.R., Relton, J.M., Slater, N.K.H., 1999. Charaterisation of a generic monoclonal antibody harvesting system for adsorption of DNA by depth filters and various membranes, Bioseperation, 8, 281–291.

Nejatishahidein, N., Zydney, A.L., 2021. Depth filtration in bioprocessing — new opportunities for an old technology. Curr. Opin. Chem. Eng. 34. https://doi.org/10.1016/j.coche.2021.100746.

Liu, H.-C., Chen, X.-Q., Duan, C.-Y., Wang, Y.-M., 2019. Failure mode and effect analysis using multi-criteria decision making methods: a systematic literature review. Comput. Ind. Eng. 135, 881–897. https://doi.org/10.1016/j.cie.2019.06.055.

Wohlenberg, O.J., Kortmann, C., Meyer, K.V., Scheper, T., Solle, D., 2022. Employing QbD strategies to assess the impact of cell viability and density on the primary recovery of monoclonal antibodies. Eng. Life Sci. 23. https://doi.org/10.1002/elsc.202200056.

Wee, H., Koo, K., Bae, E., Lee, T., 2020. Quality by design approaches to assessing the robustness of tangential flow filtration for MAb. Biologicals 63, 53–61. https://doi.org/10.1016/j.biologicals.2019.12.001.

Khanal, O., Singh, N., Traylor, S.J., Xu, X., Ghose, S., Li, Z.J., et al., 2018. Contributions of depth filter components to protein adsorption in bioprocessing. Biotechnol. Bioeng. 115, 1938–1948. https://doi.org/10.1002/bit.26707.